JGR Planets

RESEARCH ARTICLE
10.1029/2024JE008816

Evidence of 4.3 Ga Mg-Suite Magmatism in the Western Procellarum KREEP Terrane Provided by Zircon From Chang'e-5 Regolith

Chen-Long Ding[1], Alexander Nemchin[2], Xiao-Lei Wang[1], Yue Guan[1], Lan-Lan Tian[1], and Wen-Li Xie[1]

[1]State Key Laboratory of Critical Earth Material Cycling and Mineral Deposits, Frontiers Science Center for Critical Earth Material Cycling, School of Earth Sciences and Engineering, Nanjing University, Nanjing, China, [2]School of Earth and Planetary Sciences, Curtin University, Perth, WA, Australia

Key Points:

- An in situ secondary ion mass spectrometer U-Pb age of 4,311 ± 35 Ma was determined for a zircon from the Chang'e-5 lunar regolith
- Age and chemical characteristics of the ancient zircon imply that Mg-suite magmatism may be contemporaneous on the lunar nearside
- Exotic ancient zircon in the young Chang'e-5 sample provides new insights into early lunar magmatism

Correspondence to:

X.-L. Wang,
wxl@nju.edu.cn

Citation:

Ding, C.-L., Nemchin, A., Wang, X.-L., Guan, Y., Tian, L.-L., & Xie, W.-L. (2025). Evidence of 4.3 Ga Mg-suite magmatism in the western Procellarum KREEP Terrane provided by zircon from Chang'e-5 regolith. *Journal of Geophysical Research: Planets*, *130*, e2024JE008816. https://doi.org/10.1029/2024JE008816

Received 19 OCT 2024
Accepted 20 MAR 2025

Author Contributions:

Conceptualization: Alexander Nemchin, Xiao-Lei Wang
Data curation: Chen-Long Ding, Yue Guan, Lan-Lan Tian, Wen-Li Xie
Funding acquisition: Xiao-Lei Wang
Methodology: Alexander Nemchin, Xiao-Lei Wang
Project administration: Xiao-Lei Wang
Software: Chen-Long Ding, Yue Guan, Lan-Lan Tian, Wen-Li Xie
Supervision: Alexander Nemchin, Xiao-Lei Wang
Validation: Yue Guan, Lan-Lan Tian, Wen-Li Xie
Writing – original draft: Chen-Long Ding
Writing – review & editing: Chen-Long Ding, Alexander Nemchin, Xiao-Lei Wang

Abstract The formation of Mg-/Alkali-suites represents the most pronounced and oldest process in the magmatic evolution of the Moon. Fragments of these rocks have been identified among the samples collected by almost all lunar missions. In addition, remote observations indicate widespread distribution of these rocks on the Moon. However, collected samples remain restricted to the locations around the south-eastern boundary of the Procellarum KREEP Terrane (PKT), limiting the ability to confirm information provided by remote observations and to investigate relationships between Mg-/Alkali-suites in different parts of the Moon. An important feature of these rocks delivered by Apollo missions is enrichment in incompatible elements, resulting in a frequent appearance of accessory zircon, which can be considered as one of the identifiers of rocks belonging to these suites. Consequently, the age of 4,311 ± 35 Ma and chemical characteristics of a zircon grain found in an agglutinate from Chang'e-5 soil are interpreted as evidence of an origin in an Alkali or most likely Mg-suite rock. The zircon grain is exotic to the landing site surrounded by the young ca. 2.0 Ga basaltic flows and was most likely delivered to the site as a distal impact ejecta. The location of the collected sample at the Chang'e-5 landing site to the west of the Imbrium basin, remote from all other sample collection sites, confirms the wide distribution of Mg-suite rocks, at least within PKT. The age of the zircon also provides the first indication that this early magmatism could have been contemporaneous across the nearside of the Moon.

Plain Language Summary Although remote sensing observations indicate that Mg- and Alkali-suite rocks are widely distributed on the Moon, the samples returned by Apollo missions are confined to the lower latitude regions on the lunar nearside. This limits our ability to determine whether the formation of these rocks on the Moon was widespread and confined to a specific time period. China's Chang'e-5 mission extended the areal distribution of available samples. Here we report a zircon grain with an ancient age (ca. 4.3 Ga) and geochemistry that clearly distinguishes it from other Chang'e-5 mineral and rock fragments that are typically related to the basalt surrounding the landing site and imply its affinity to lunar Alkali-suite or most likely Mg-suite rocks. A later impact may have delivered materials from the adjacent highlands or ancient ejecta to the Chang'e-5 sampling site where the young basalts are located. This zircon provides evidence of early contemporaneous Mg-suite magmatism across the nearside of the Moon.

1. Introduction

Mg-suite and Alkali-suite rocks are viewed to represent the products of the first stage of lunar crust building following initial differentiation of the Moon during Lunar Magma Ocean (LMO) crystallization (Borg et al., 2020; Elardo et al., 2020; Shearer & Papike, 2005; Shearer et al., 2015). These rocks appear to be plutonic to hypabyssal and are believed to have crystallized as layered intrusions akin to those found on Earth, although available lunar samples do not provide any clear evidence of layering (Hess, 1994; Raedeke & Mccallum, 1984; Shearer & Papike, 2005; Shearer et al., 2015). Known Mg-suite samples include variety of rocks such as dunites, troctolites, norites, gabbro-norites, anorthositic troctolites and anorthositic norites and in some cases granites (Hess, 1994; Papike et al., 1996, 1998; Shearer & Papike, 2005; Shearer et al., 2015). Nevertheless, they all are characterized by high Mg# and concentrations of some incompatible elements such as rare earth elements (REE) and low concentrations of alkali elements as well as Ni, Co and Cr (Hess, 1994; Papike et al., 1996, 1998; Shearer & Papike, 2005; Shearer et al., 2015). These chemical features indicate contribution from three contrasting components, which are, high Mg# early cumulates of LMO, anorthosite from the early crust and, at least for the

samples delivered by various sample return missions, KREEP (for high K, REE, and P), although recent studies of lunar meteorites potentially representing broader sampling of the Moon have found that some high Mg rocks do not have accompanying high REE concentrations, leading to suggestion that KREEP signature of Mg-suite samples may be localized and confined to the Procellarum KREEP Terrane (PKT) (Elardo & Astudillo Manosalva, 2023; Gross et al., 2020). Regardless, the contrasting chemical characteristics of these samples also resulted in the existing range of petrogenetic models used to explain formation of Mg-suite rocks, although most of these models invoke gravitational mantle overturn postdating LMO crystallization as a mechanism for bringing different components together (Elardo et al., 2011; Hess, 1994; Longhi & Boudreau, 1979; Shearer & Papike, 2005; Shearer et al., 2015; Taylor et al., 1993). Alkali-suite consists of alkali anorthosite, mafic alkali rocks (norite, gabbro, and gabbronorite), KREEP basalt and quartz monzodiorite (QMD) (Papike et al., 1998). In addition, some small fragments of felsic rocks have been observed in Apollo breccia samples (Meyer et al., 1996; Papike et al., 1998; Shih et al., 1985) and could be included in this suite of rocks. Chemical characteristics of these rocks include enrichment in alkali metals and other incompatible elements, including REEs (Papike et al., 1998; Snyder et al., 1995). As a result, the origin of these rocks is commonly linked to KREEP rich reservoirs on the Moon (Shervais & McGee, 1999; Snyder et al., 1995).

Large samples of Mg- and Alkali-suite rocks exceeding a few grams in weight are rare (Dymek et al., 1975; Papike et al., 1998; Shearer et al., 2015; Warren & Wasson, 1978). Most of the available Mg- and Alkali-suite samples in the Apollo collection have been found to be less than 1 g and are often included as clasts in breccias (Papike et al., 1998). However, they are present at all landing sites with the possible exception of Apollo 11 (He et al., 2024; Papike et al., 1998; Shearer & Papike, 2005). The majority of Mg-suite rocks appear in Apollo 17 samples while Alkali-suite fragments are most common in Apollo 14 and to a lesser degree in Apollo 15 and 12 samples (Papike et al., 1998; Shearer et al., 2015; Shervais & McGee, 1999). Nevertheless, remote observations indicate potentially widespread distribution of both Mg- and Alkali-suite materials around the lunar surface (Klima et al., 2011, 2013; Moriarty et al., 2021; Pieters et al., 2011), especially if recordings of Mg-spinel occurrences are taken into account (Dhingra et al., 2011), suggesting that the early plutonic magmatism on the Moon may be a global phenomenon. However, temporal relationships between different expressions of such type of magmatism remain unclear due to the lack of available age dates (Borg & Carlson, 2023; Borg et al., 2015), which are also confined to the eastern to south-eastern part of the PKT. A dozen of large Mg- and Alkali-suite samples have been analyzed for Sm-Nd isotope systems that are considered least prone to post-formation resetting (Borg et al., 2015, 2020; Carlson & Lugmair, 1981), with the results indicating that the time of formation of both suites is mostly in the range from about 4.35 Ga to about 4.10 Ga (Borg & Carlson, 2023; Borg et al., 2020; Carlson & Lugmair, 1981). The earlier-mentioned enrichment of Mg- and Alkali-suite rocks in incompatible elements (Shearer et al., 2015; Snyder et al., 1995) also leads to a common presence of Zr-rich accessory minerals in these rocks, including zircon. As zircon is one of the minerals most used for chronology (Hoskin & Schaltegger, 2003), utilizing its U-Pb system can help to expand the total number of samples with determined ages to a population of small (mm size) fragments found in breccia samples (Crow et al., 2017; Nemchin et al., 2009; Pidgeon et al., 2007; A.-C. Zhang et al., 2011, 2012), especially fragments of Alkali-suite rocks (Meyer et al., 1996). In addition, Mg- and Alkali-suite rocks appear to be the only types of samples on the Moon that consistently show the presence of easily identifiable quantities of zircon (Meyer et al., 1996; Nemchin et al., 2008; B. Zhang, Lin, Moser, Warren, et al., 2021), although three zircon grains were identified in Chang'e-5 basalt fragment and one in an agglutinate fragment (Zhou et al., 2023). Their young age (ca. 2,036 ± 19 Ma) indicates that the grains are likely the product of extreme fractionation of Chang'e-5 basalt melt (Zhou et al., 2023). Nevertheless, zircon appears to be rare in mare basalts as this mineral has not been identified so far in any of Apollo mare basalts. Consequently, it is highly likely that the population of a few hundred zircon grains found as mineral fragments and analyzed in Apollo breccias mostly represent temporal distribution of the Mg- and Alkali- rock suites and their ages reflect timing of lunar plutonic magmatism, even though these grains have lost petrologic link to their host rocks. Nevertheless, even if all available chronological information is combined, it only characterizes a relatively small area of PKT covered by Apollo landing sites (Borg & Carlson, 2023; Shearer et al., 2015) and dating of samples from other locations is required to confirm that temporal patterns of plutonic magmatism are consistent across the larger PKT and Moon in general. One of the opportunities to expand the areal coverage of chronological data is provided by the samples delivered by the recent Chang'e-5 (CE-5) mission. Even though these samples are largely representative of relatively young mare basalt units (Boschi et al., 2023; Che et al., 2021; Q.-L. Li et al., 2021), several occurrences of exotic rock fragments have been described in the literature (He et al., 2024; Zeng et al., 2023).

The aim of this study was to present new data for another zircon grain from Chang'e-5 sample. Its ancient age and chemical characteristics indicate a link to the early (ca. 4.3 Ga) plutonic magmatism on the Moon, providing the first step in assessing temporal variability of this magmatism in the wider PKT.

2. Materials and Methods

2.1. Sample Preparation and Scanning Electron Microscopy

The Chang'e-5 regolith sample CE5C0600YJFM00501 was provided by the China National Space Administration (CNSA). The fragments were picked up, embedded in epoxy mounts and polished at Nanjing University. Structures and internal compositions of different fragments were analyzed using an Oxford AZtec X-Max 150 X-ray energy dispersive spectrometer (EDS) detector attached to a Carl Zeiss-Supra55 Field emission scanning electron microscope (FESEM). High-resolution backscattered electron (BSE) images and the secondary electron (SE) images were captured using 15 and 7 kV acceleration voltage separately with a working distance of ~8.5 mm. The EDS data of different minerals were obtained using 15 kV acceleration voltage. A zircon grain was discovered in an agglutinate during SEM imaging. The cathodoluminescence (CL) image of the zircon grain was obtained using the CL detector attached to a TESCAN Mira3 FESEM at Nanjing Hongchuang Geological Exploration Technology Service Co., Ltd using a 7 kV acceleration voltage with a working distance of 13 mm in order to observe the microstructure of the zircon prior to SIMS analysis.

2.2. Major Element Analysis of Minerals

Major element compositions of pyroxene and plagioclase were determined using an electron probe microanalysis utilizing JEOL JXA-8230 at the State Key Laboratory of Critical Earth Material Cycling and Mineral Deposits, Nanjing University. Quantitative analyses of the minerals were conducted using a 1 μm spot for pyroxene and 3 μm for plagioclase with 20 nA electron beam current and a 15 kV accelerating voltage. Natural minerals and synthetic glasses were used as standards, and the detection limits for most elements were 0.01–0.03 wt.%. Matrix corrections were based on ZAF procedures.

2.3. Zircon U-Pb Dating

Measurements of U, Th and Pb isotopes in the zircon were conducted using a CAMECA IMS-1300HR^3 SIMS at the State Key Laboratory of Critical Earth Material Cycling and Mineral Deposits, Nanjing University. Before analysis, each analytical spot was pre-sputtered for 120 s with a 5 nA primary beam of $^{16}O^-$ to remove the gold coating using a 5,000 μm field aperture in order to minimize possible surface contamination. The ion images of $^{90}Zr_2{}^{16}O^+$ on a 10 μm × 10 μm area were used to precisely locate the target. A Gaussian illumination mode was used to focus a primary beam of $^{16}O^-$ to a size of 4 μm with the intensity kept around 500 pA. The mass spectrometer was operated at a mass resolution power (MRP) of 7,000 (50% peak height) with a 65 μm entrance slit to resolve Pb from molecular interferences. Secondary ions with 10 kV energy were detected using electron multiplier (EM), with masses $^{90}Zr_2{}^{16}O^+$, $^{92}Zr_2{}^{16}O^+$, 200.5 (background), $^{94}Zr_2{}^{16}O^+$ (reference of $^{204}Pb^+$), $^{204}Pb^+$, $^{206}Pb^+$, $^{207}Pb^+$, $^{208}Pb^+$, $^{232}Th^{16}O^+$, $^{238}U^{16}O^+$, $^{238}U^{16}O_2{}^+$ analyzed sequentially by stepping of the magnet field in the mono-collection mode. The signal of $^{90}Zr_2{}^{16}O^+$ was used for peak-centering. Each measurement consists of 12 cycles with a total analytical time of about 23 min. Zircon standard 91500 was utilized to calibrate the Pb/U ratio as well as U and Th concentrations (Wiedenbeck et al., 1995). Given the low common Pb of the analyzed zircon, correction of ratios for common Pb was based on measured ^{204}Pb and assumed this to be modern terrestrial Pb contamination on the surface, with a composition corresponding to the model terrestrial Pb (Stacey & Kramers, 1975). The monitoring standard Temora-2 zircon has a concordia age of 421 ± 11 Ma and a $^{206}Pb/^{238}U$ weighted average age of 422 ± 7 Ma, which agrees with the ID-TIMS age (416.78 ± 0.33 Ma) within the uncertainties (Black et al., 2004).

2.4. Trace Element Analysis of Zircon

Trace element concentrations of the zircon were analyzed using a high-resolution CAMECA IMS-1300HR^3 instrument at the State Key Laboratory of Critical Earth Material Cycling and Mineral Deposits, Nanjing University. To minimize possible surface contamination, a 5 nA primary beam with 20 μm raster was used for each analytical spot to remove the gold coating prior to analyses. A Gaussian illumination mode was used to focus a primary beam of $^{16}O^-$ to a size of 5 μm with the intensity kept around 600 pA. In order to separate the light-REE

oxide interference, the mass spectrometer was operated at a mass resolution power (MRP) of 15000 with a 40 μm entrance slit and 85 μm exit slit. Secondary ions with 10 kV energy were detected in the mono-collector mode and the following mass sequence was measured: $^{48}Ti^{16}O^+$, $^{28}Si_2{}^{16}O^+$, $^{89}Y^+$, $^{139}La^+$, $^{140}Ce^+$, $^{141}Pr^+$, $^{142}Nd^+$, $^{147}Sm^+$, $^{153}Eu^+$, $^{158}Gd^+$, $^{159}Tb^+$, $^{163}Dy^+$, $^{165}Ho^+$, $^{167}Er^+$, $^{169}Tm^+$, $^{174}Yb^+$, $^{175}Lu^+$, and $^{178}Hf^+$. Each spot analysis included 5 cycles with a total analytical time of about 20 min. The synthetic glass standard NIST-610 was used to find peak positions. Element concentrations were standardized against the NIST-612 (light-REE) (Jochum et al., 2005) and zircon 91500 standard (Coble et al., 2018), which were analyzed repeatedly throughout the duration of the analytical session. Intensities were normalized to $^{28}Si_2{}^{16}O^+$ and stoichiometric compositions were assumed for zircon standards and unknowns. The synthetic glass standards NIST-610, NIST-612 and zircon standard Tanz (Hu et al., 2021) were used to monitor the reproducibility of the data as well as instrument stability.

2.5. Zircon Ti Concentration Analysis and Ti Temperature Calculation

The Ti concentration of the zircon was obtained using an ion imaging approach (Harrison & Schmitt, 2007) to avoid the influence of potential inclusions and glass surrounding the zircon grain. Three regions of the sample were selected to obtain the ratio of $^{48}Ti^+/^{90}Zr^+$. Before analysis, a 5 nA primary beam with 20 × 20 μm raster was used to remove the goad coating and clean the surface of the sample. A Gaussian illumination mode was used to focus a primary beam of $^{16}O^-$ with the intensity kept around 50 pA to acquire the ion images of $^{48}Ti^+$ and $^{90}Zr^+$. The final work beam size is <2 μm and with 5 × 5 μm raster. The mass spectrometer was operated at a mass resolution power (MRP) of 15,000 (50% peak height) with a 40 μm entrance slit and 80 μm exit slit. Hence, the interference $^{48}Ca^+$ can be separated from the $^{48}Ti^+$ at less than 50% intensity (Harrison & Schmitt, 2007). The analyses were conducted using electron multiplier (EM) in the mono-collection mode, which includes 10 cycles and a total integration time for $^{48}Ti^+$ of 100 s. Titanium counts ($^{48}Ti^+$) were normalized to counts of $^{90}Zr^+$. All image files containing raw intensities in 128 × 128 pixels were processed using Winimage software provided during CAMECA initial installation. Zircon standard 91500 was used to calibrate the Ti concentration of the sample. The zircon standard Tanz was used to monitor the reproducibility of the data as well as instrument stability.

3. Results

3.1. Petrographic Characteristics and Mineral Compositions

The zircon grain was discovered in an agglutinate fragment that contains clinopyroxene, plagioclase and ilmenite clasts varying in size from a few to about 50 microns and surrounded by glass, which also contains numerous vesicles (Figure 1a; Table S1 in Ding et al. (2025)). The grain shows euhedral terminations on one side and curved boundaries on the other, indicating that it is probably a broken fragment (Figure 1b). It is a separate piece about 17 μm × 8 μm fully surrounded by glass but located next to a large (~50 microns in length) clinopyroxene grain. Plagioclase is visible at one edge of this clinopyroxene grain (Figure 1a). The compositions of pyroxene ($En_{10.2\text{-}37.5}Fs_{28.3\text{-}67.0}Wo_{18.0\text{-}39.6}$) and plagioclase ($An_{78.4\text{-}80.7}$) fall within the range of CE-5 basalt mineral compositions and show similar evolutionary trends (Figure 2). The zircon shows simple internal structure with a few weak parallel bands in the CL image (Figure 1c), and no zonation in the BSE and SE images (Figures 1b and 1d). In addition, this zircon grain lacks obvious micro-textural features indicative of shock alteration.

3.2. Zircon U-Pb Age

Three U-Pb isotope spot analyses (Table S2 in Ding et al. (2025) and Figure 3) of the zircon indicate U and Th concentrations of 30–40 ppm and 11–15 ppm, respectively, and a limited variation of Th/U ratio (mean value of 0.39), consistent with the data for reported lunar zircon (Crow et al., 2017; Trail et al., 2020). The analyses show slight Pb loss, forming a discordia line with an upper intercept of 4,311 ± 35 Ma (MSWD = 0.013, probability of the fit = 0.91) (Figure 3a). They also showed consistent $^{207}Pb/^{206}Pb$ dates, yielding a mean age of 4,299 ± 12 Ma (MSWD = 0.32) (Figure 3b). The age is significantly older than the Pb-Pb ages of local basalts at the CE-5 sampling site (Boschi et al., 2023; Che et al., 2021; Q.-L. Li et al., 2021) and the zircon grains recently found in the CE-5 samples (Zhou et al., 2023). The mentioned slight discordance of the analyses suggesting possible small level of Pb loss could be associated with the event responsible for the zircon transportation to the landing site, although the lower intercept of discordia is defined with a very large uncertainty not allowing placing accurate limits on the timing of this event.

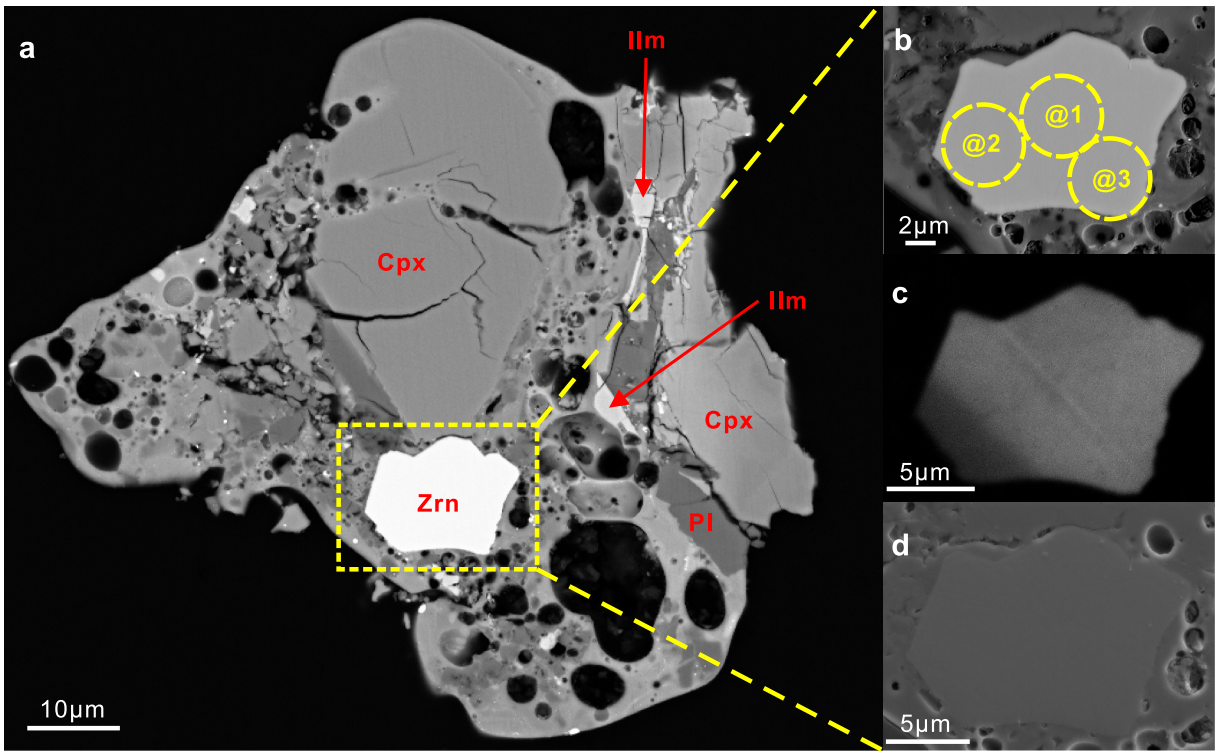

Figure 1. SEM images of the zircon-bearing fragment from CE5C0600YJFM00501. (a) BSE image of the agglutinate fragment. Cpx—clinopyroxene, Pl—plagioclase, Ilm—ilmenite, Zrn—zircon. (b) BSE image of zircon grain showing no obvious internal microstructures. Yellow circles show the locations of U-Pb analytical spots. (c) and (d) CL and SE images of zircon. The CL image shows weak zoning inside the grain.

3.3. Trace Elements of the Zircon

The trace elements, including REE, Y, and Hf were analyzed in two spots within zircon grain (Table S3 in Ding et al. (2025)). The obtained chondrite-normalized REE concentrations show typical steep patterns of zircon, with light REE (LREE) a few times and heavy REE (HREE) a few thousand times higher than chondrite as well as an

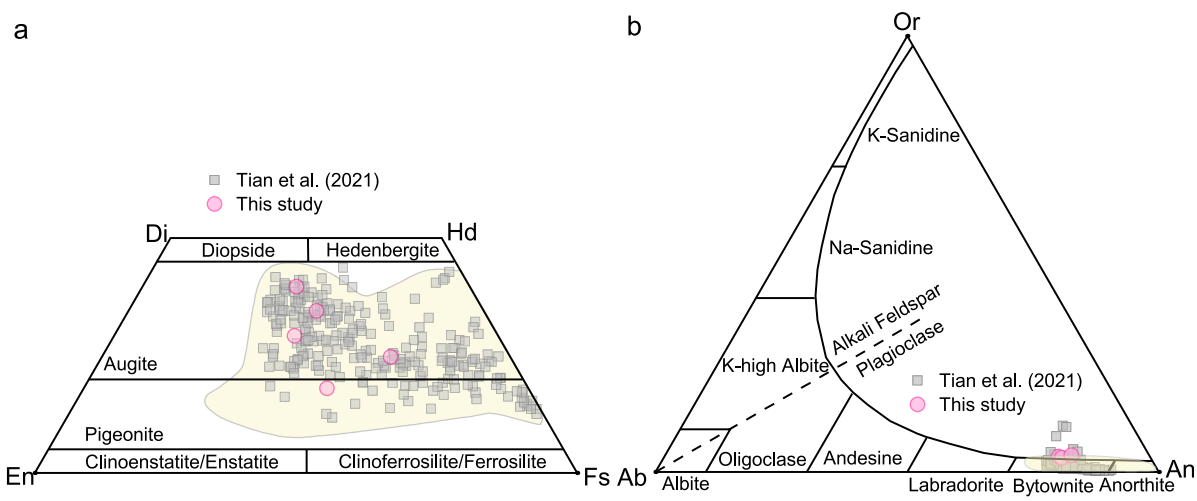

Figure 2. Compositions of pyroxene and plagioclase from investigated agglutinate fragment from CE5C0600YJFM00501. (a) The pyroxene quadrilateral diagram comparing the pyroxene analyses in CE-5 basalts (C. Li et al., 2022; Tian et al., 2021) to the pyroxene in the investigated agglutinate fragment. (b) Ab-An-Or diagram comparing feldspar compositions in CE-5 basalts (C. Li et al., 2022; Tian et al., 2021) to those in agglutinate fragment. The yellow fields in (a) and (b) show the full range of mineral compositions in CE-5 (C. Li et al., 2022). Similar compositions and evolutionary trends suggest that the minerals in the agglutinate are derived from CE-5 local basalts rather than from the zircon's host rock. The results are shown in Table S1 in Ding et al. (2025).

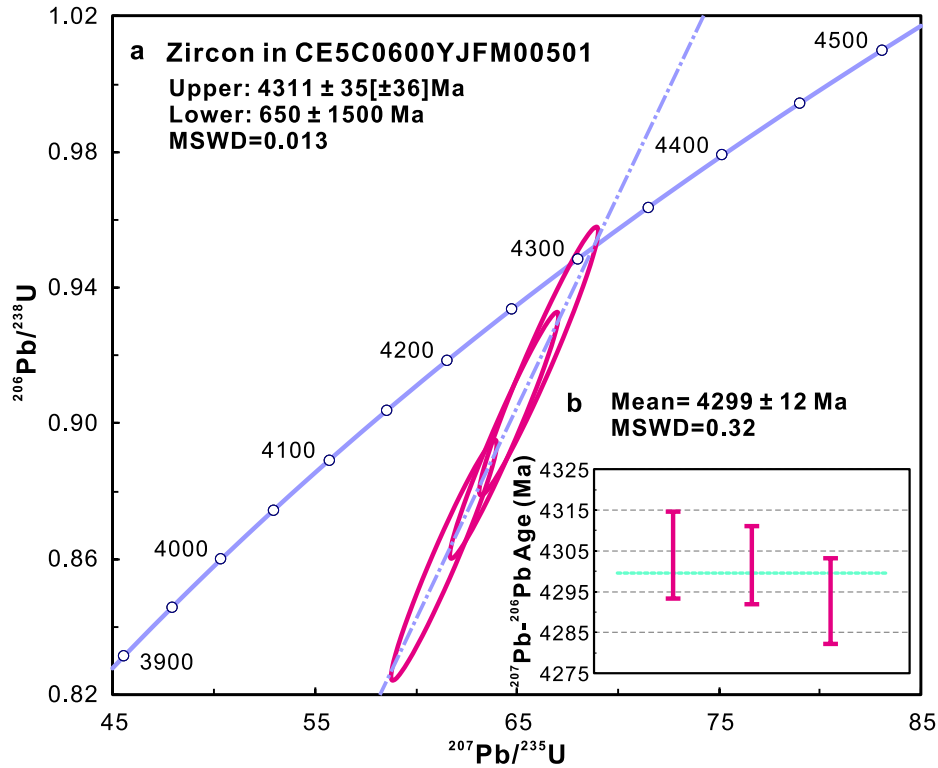

Figure 3. Concordia diagram showing U-Pb data obtained for the lunar zircon in CE5C0600YJFM00501. (a) Three spot analyses of the zircon yield an upper intercept age of 4,311 ± 35 Ma (2σ). (b) ^{207}Pb-^{206}Pb weighted average age is 4,299 ± 12 Ma (2σ).

evident negative Eu anomaly, similar to those reported in Apollo zircon with the exception of three LREEs (Figure 4a) (Crow et al., 2017; Trail et al., 2020). The calculated chondrite-normalized REE values from Nd to Lu of parent magma show a pattern with a slightly negative slope where LREE are 30–50 times and HREE about 10–20 times higher than chondrite, and a pronounced negative Eu anomaly (Figures 4b–4f). The concentrations of La, Ce and Pr are clearly elevated in the investigated zircon grain compared to Apollo zircons, which is likely the result of partial overlap of analytical spots on the glass surrounding zircon (Figure 4a). As LREE concentrations in zircon are up to four orders of magnitude lower than those of the HREEs, they are susceptible to be influenced by contamination (Hinton & Upton, 1991). Crow et al. (2017) had assessed the effects of contamination on trace element analysis of lunar zircons. They suggested that the studied lunar zircons had a range of potential sources of REE contamination, including impact melt inclusions, cracks, annealed fractures, or regions between zircon and impact melt. Their observations indicate that small amounts of impact melt glass can readily produce the variations in LREE patterns, which are similar to those observed in CE-5 agglutinate zircon (Figure 4a). Furthermore, assuming that the agglutinate glass composition is similar to that of the basalt surrounding Chang'e-5 landing site (Figure 4b), LREE concentrations of this glass are expected to be three orders of magnitude higher than those commonly observed in zircon, while HREE concentrations are generally similar or even lower than those in zircon grains. As a result, any small addition of glass within the analytical spot will drastically increase estimated LREE concentration of zircon, while having no visible effect on HREE. However, neither BSE, SE nor CL imaging of investigated zircon taken prior to chemical and isotopic analyses indicate presence of fractures or inclusions at the polished surface of the grain (Figures 1b–1d), post analyses imaging indicates that spot TE@2 (Figure 4a) may overlap zircon grain boundary and partially include surrounding glass. The spot TE@1 appears to be confined fully within zircon grain and also shows a lesser degree of flattening of the LREE part of the pattern. However, the possibility of encountering some imperfections during the analysis cannot be fully excluded even for this spot. Taking the similar possibility of an overlap of analytical spots during Ti analyses into account and to avoid the possible influence of the surrounding glass, we determined Ti concentrations in the zircon grain using the SIMS Ti imaging approach (Harrison & Schmitt, 2007) (Figure 5; Table S4 in Ding et al. (2025)). These

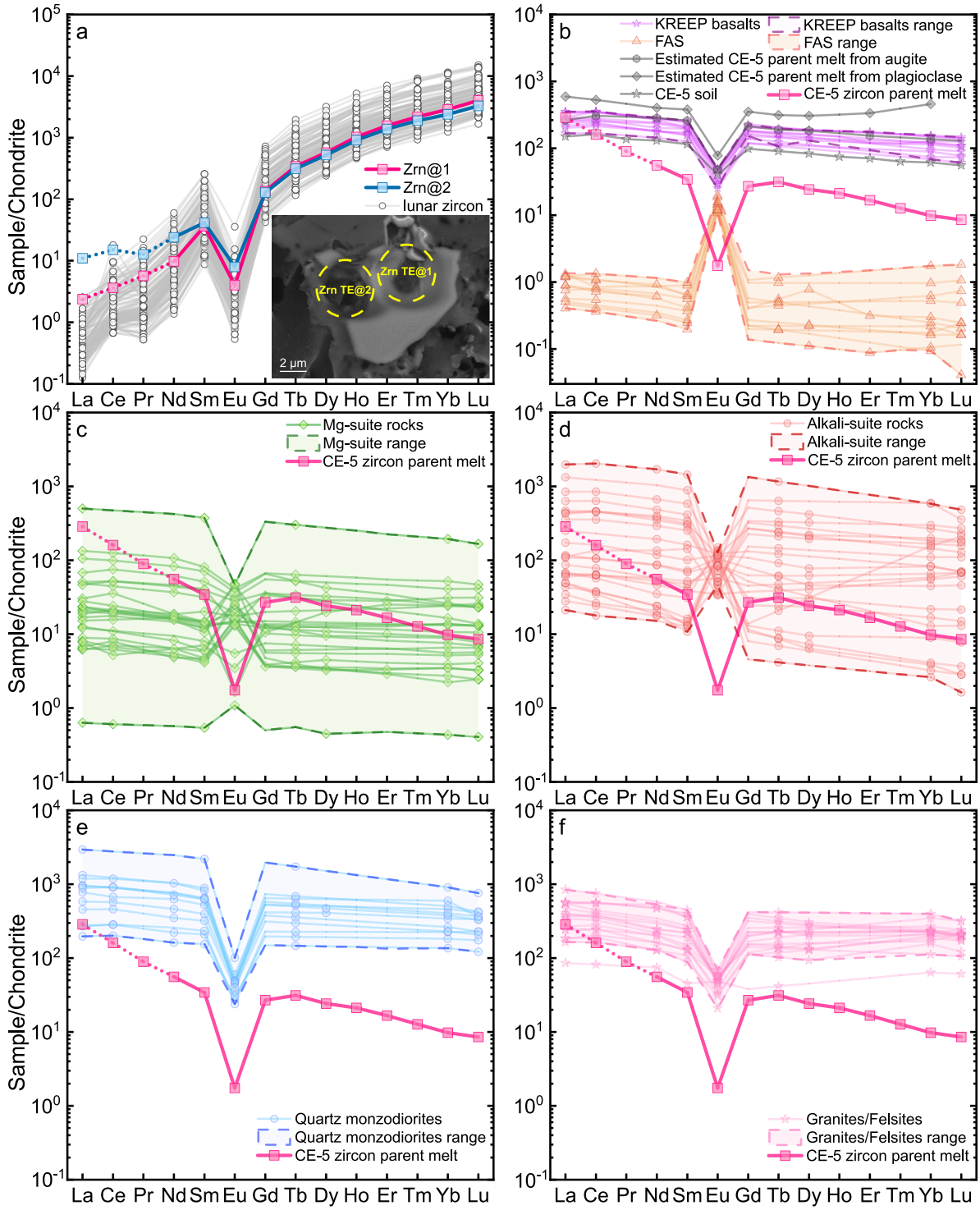

Figure 4. The chondrite normalized REE patterns of the CE-5 zircon and its estimated parent melt. (a) Comparison of chondrite-normalized REE concentrations of the zircon in CE-5 agglutinate and lunar zircon in Apollo samples. The locations of the SIMS measurement spots are marked on the BSE image with yellow dashed circles. (b–f) The REE concentrations in the calculated parent melt of CE-5 agglutinate zircon, CE-5 basalt and soil, and the major lunar plutonic rock types (Papike et al., 1998). (b) CE-5 basalt and soil data from Tian et al. (2023) and Zong et al. (2022). (c–f) Mg-suite rocks, Alkali-suite rocks, quartz monzodiorites, granites/felsites, from Papike et al. (1998). The estimated parent melt has a distinct negative Eu anomaly, with REE content an order of magnitude below that of KREEP and within the range of Mg-/Alkali-suite rocks. CI chondrite values are from McDonough and Sun (1995).

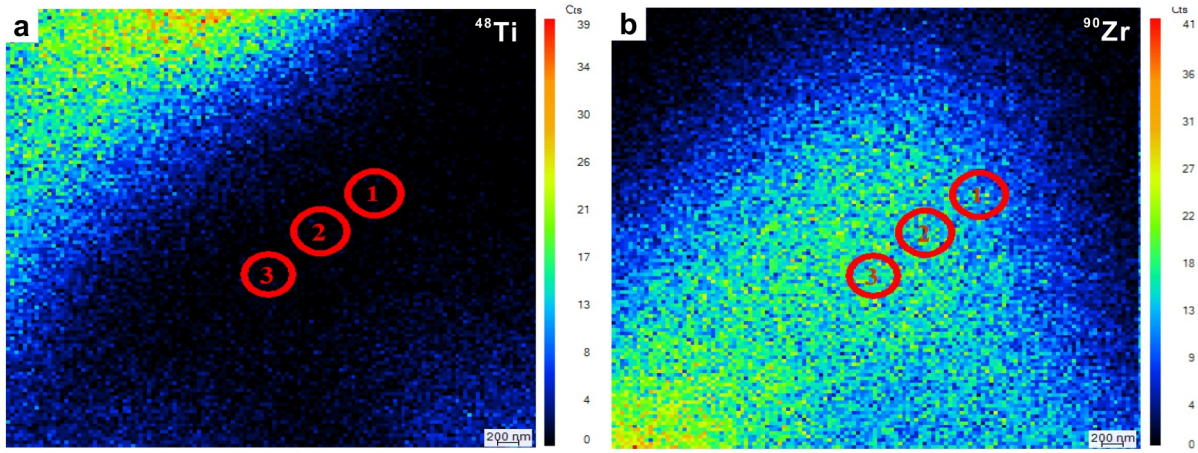

Figure 5. The ion images of the zircon and surrounding areas used to determine the concentration of Ti. (a) The ion signal of ^{48}Ti. (b) The ion signal of ^{90}Zr. Red circles represent regions of interest used to estimate Ti concentrations. The results are shown in Table S4 in Ding et al. (2025).

detected concentrations range from 189 to 229 ppm and define an average temperature for zircon crystallization of 1,324 ± 89°C, using the activities of TiO_2 and SiO_2 defined by Crow et al. (2017). Using a different approach to estimate TiO_2 and SiO_2 activities (Trail et al., 2020) results in a slightly lower crystallization temperature of 1,144 ± 68°C. Both estimates, however, are higher than those temperatures commonly determined for terrestrial zircons (Carley et al., 2022; C.B. Keller et al., 2017).

4. Discussion

4.1. Possible Host Rocks for the CE-5 Zircon

The old age of the zircon grain (ca. 4,311 ± 35 Ma) investigated here clearly sets it apart from rare zircon grains recorded previously in CE-5 samples, which were interpreted to be the product of extreme fractionation of CE-5 basalt melt (Zhou et al., 2023). It also indicates that this old zircon is not formed in CE-5 mare basalt with the age of about 2 Ga (Boschi et al., 2023; Che et al., 2021; Q.-L. Li et al., 2021) but crystallized in a rock distant to the landing area and was transported to the collection site by one or several later impacts. The age of the investigated zircon is consistent with the ages of zircon grains reported in the Apollo samples, which appear to record multiple episodes of magmatic activity before 4,000 Ma (Nemchin et al., 2008) and show an age peak around 4,330–4,350 Ma (Barboni et al., 2024; Borg & Carlson, 2023). This peak is at the lower limit of estimated formation time of some LMO cumulates and coincides with ages determined for several Mg-suite rocks (Borg & Carlson, 2023; Borg et al., 2015). Therefore, the zircon studied here is likely to have an origin similar to that of multiple zircon grains from Apollo samples, preserving a record of an early large-scale magmatism and lunar crust construction on the Moon.

Although many of analyzed Apollo zircon grains are found as mineral clasts in impact melt breccia samples with no clearly established link to their host (Bellucci et al., 2019; Crow et al., 2017; Grange, Nemchin, & Pidgeon, 2013; Nemchin et al., 2008; Vanderliek et al., 2021; A.-C. Zhang et al., 2011, 2012), they are commonly interpreted as formed in Mg/Alkali-suite rocks, implying a large-scale magmatic episode(s) responsible for building crust on the lunar nearside (Borg & Carlson, 2023; Crow et al., 2017; Grange, Nemchin, & Pidgeon, 2013; Meyer et al., 1996; Thiessen et al., 2019). The main reason for this link between zircon occurrences and Mg/Alkali-suite rocks is that zircon crystallization requires zircon saturation in the magma, which is difficult to achieve in mafic melts (Dickinson & Hess, 1982), unless they are initially enriched in incompatible elements including Zr, which is the case for lunar Mg/Alkali-suite rocks (Papike et al., 1998; Shearer et al., 2015). There are also some zircon grains described in the previous studies that are either part of lithic clasts found in the breccias or attached to rock forming minerals (Grange, Nemchin, & Pidgeon, 2013; Meyer et al., 1996; Nemchin et al., 2008; Thiessen et al., 2019; A.-C. Zhang et al., 2012) allowing direct identification of their host rock. Many are associated with felsites, "granites" and granophyres containing two feldspars and silica in addition to zircon grains (Grange, Nemchin, & Pidgeon, 2013; Meyer et al., 1996; Nemchin et al., 2008; Zeng et al., 2020; A.-C.

Zhang et al., 2012). There are also several occurrences of zircon in the lithic clasts composed of two feldspars, clinopyroxene and silica, which are likely to represent quartz monzonite diorite (QMD) rocks forming part of Alkali-suite (Grange, Nemchin, & Pidgeon, 2013; Meyer et al., 1996) and more common rock fragments of norite and noritic anorthosite composition (Grange, Nemchin, & Pidgeon, 2013; Nemchin et al., 2008; Thiessen et al., 2019) which could belong to both Alkali and Mg-suites. Nevertheless, at least two zircon grains have been identified by Meyer et al. (1991) in the fragments that clearly belong to Mg-suite. One was identified in the thin section 14303, 52 and in addition to zircon contains olivine as well as low- and high-Ca pyroxene. The other is troctolite found in the thin section 14306, 150 (Meyer et al., 1991). In addition, some zircons have been identified in the thin section 78238, 14 which contains dominant cumulus plagioclase and orthopyroxene (B. Zhang, Lin, Moser, Warren, et al., 2021) and two thin sections of 72255 Civet Cat norite clast (B. Zhang, Lin, Moser, Hao, et al., 2021).

Published data indicate that zircon can form in the samples covering a full range of rock types that belong to both Alkali and Mg-suites (Meyer et al., 1991). A number of clasts of different rock forming minerals are present in the investigated agglutinate fragment. However, zircon grain is not directly attached to any of these clasts and is surrounded by glass (Figure 1). The compositions of the clasts link them to the CE-5 basalt, suggesting that the zircon was probably added to the reworked local basalt components as a result of regolith mixing postdating both zircon and basalt formation (Figure 2). Therefore, none of these minerals can be used to define zircon's original host rock and the clues about zircon's origin must come from the age and chemistry of zircon itself.

In addition to age, evidence of resemblance between the zircon grain analyzed here and previously investigated Apollo zircon occurrences is provided by their chemical similarity. Since the first publication that utilized Ti in zircon thermometry (Watson & Harrison, 2005), a number of studies highlighted dependence of temperature obtained from Ti concentrations in zircon on the activity of SiO_2 and TiO_2 in the parent magma (Crow et al., 2017; Trail et al., 2020). The best estimates of αSiO_2 and αTiO_2 given by Crow et al. (2017) and using MELTS simulations are 0.6 ± 0.1 and 0.25 ± 0.05 respectively. Trail et al. (2020) suggested range of αSiO_2 of 0.45–1 and αTiO_2 values of 0.45 to 0.65 for lunar zircons. They also noted that the variation of temperature estimates is within 70°C when the difference between αSiO_2 and αTiO_2 is less than 0.3. In any case, both methods imply a significantly higher crystallization temperature for zircon in CE-5 agglutinate than those usually determined for terrestrial zircons (Carley et al., 2022; C.B. Keller et al., 2017). High temperature estimates based on Ti concentrations (Crow et al., 2017; Trail et al., 2020; Watson & Harrison, 2005) obtained in the studied grain and absence of definitive oscillatory zoning normally observed in terrestrial magmatic zircons (Hinton & Upton, 1991; Hoskin & Schaltegger, 2003), but rarely seen in lunar zircon grains indicates that the parent melts are likely to be Mg-rich, anhydrous and of high solidus temperature as well as low viscosities (Grange, Pidgeon, et al., 2013; Mattinson et al., 1996).

Additional arguments for Mg-/Alkali-suite origin of the investigated zircon grain come from the calculation of REE concentrations in the melt coexisting with the grain based on observed zircon concentrations and existing partition coefficients (Hinton & Upton, 1991; Nemchin et al., 2010). As noted earlier, lightest REE (La, Ce, Pr) concentrations appear to be overestimated most likely as a result of the presence of phases other than zircon within analytical spots. Consequently, only REEs heavier than Pr are suitable for comparison of estimated REE patterns of melt coexisting with this zircon and REE patterns of known Mg/Alkali-suite rocks. The calculated melt REE enrichment relative to chondrite clearly differentiates it from many other products of LMO crystallization and lunar magmatism, such as KREEP basalts, ferroan anorthosite suite (FAS) (Papike et al., 1998) and CE-5 basalt (Tian et al., 2023; Zong et al., 2022) (Figure 4b). It is also apparent that lunar granite/felsite samples, QMD and most of Alkali-suite gabbros and norites are more enriched in REE compared to the calculated composition of the melt coexisting with investigated zircon (Papike et al., 1998) (Figures 4d–4f). The observed pattern is also different from LREE depleted patterns determined for the melt inclusions in zircon recovered from meteorite NWA10049 (Zeng et al., 2020) and interpreted to crystallize from silica rich fraction of immiscible melt. This zircon occurs as a clast in a meteorite breccia matrix and lacks petrographic context. Although some Alkali-suite norites and anorthosites appear to have similar levels of enrichment, anorthosites show pronounced positive Eu anomalies (Figure 4d), making these rocks an unlikely source of zircon grain investigated here.

In contrast, the REE pattern of the calculated melt is in the middle of the observed range recorded for Mg-suite rocks, if the most REE rich sample 14161, 7044 is considered (Figure 4c). This sample, however, is a fragment extracted from 2 to 4 mm size fraction of Apollo 14 soil sample, which is enriched in phosphates and contains

zircon as well as K-feldspar (Jolliff et al., 1993). Although it is commonly included in published compilations of Mg-suite rocks, it is possible that it is enriched in the late mesostasis and is not representative for REE estimation of the larger rock sample. If this sample is excluded, the REE pattern of the melt coexisting with Chang'e-5 zircon analyzed here would correspond to those of some of the most enriched Mg-suite rocks (Figure 4c). However, Mg-suite rocks usually show a small positive to negative Eu anomaly or its absence, which also appears to be different from the pattern calculated for the melt coexisting with the zircon grain (Figure 4c). Nevertheless, zircon is likely to appear very late in the mafic magma crystallization sequence when zircon saturation is reached and the majority of rock forming minerals are crystallized (Dickinson & Hess, 1982; Zhou et al., 2023). At this point melt composition could be different from the starting composition and Eu concentrations (as well as Eu anomaly) in particular could be defined by proportion of plagioclase already crystallized at time of zircon crystallization. Consequently, while the chemical characteristics of the grain appear to be more compatible with its formation in a Mg-suite rock, Alkali-suite rocks can not be completely dismissed as a possible source of investigated zircon.

4.2. Possible Location of the Host Rock

It is important to note that exotic clasts have been found in many if not all Apollo soil samples (Korotev et al., 2011; Papike et al., 1982; Simon et al., 1983, 1985, 1988). Several explanations for the presence of Mg-suite rocks and/or the ancient zircon grain that appear to originate in these rocks in CE-5 soil samples are possible with various levels of probability. One is an excavation of these materials if they are present in the sequences underlying CE-5 basalt unit (Em4) by one of the local impacts postdating formation of this unit. However, this appears to be the least probable option as the estimated thickness of young basalts in the area is about 50 m and remote sensing indicates that these young basalts overlay older basaltic units (Em3) with an estimated thickness of 900 m (He et al., 2024; Qian, Xiao, Head, Wöhler, et al., 2021). Consequently, only impacts forming craters of at least several kilometers in size are expected to excavate basement containing rocks with age comparable to that of zircon investigated here and there is only one crater of about 5 km within the area covered by CE-5 basalt unit (Qian, Xiao, Head, Wöhler, et al., 2021). However, a relatively thin (∼10 m) paleo-regolith layer has been proposed to exist directly under CE-5 basalt unit and this paleo-regolith can contain materials representing a much earlier history of the Moon and can be excavated by smaller impacts (He et al., 2024; Hou et al., 2022; Qian, Xiao, Head, Bogert, et al., 2021; Qian, Xiao, Head, Wöhler, et al., 2021; Qian, Xiao, Wang, et al., 2021; Xie et al., 2020). This layer of paleo-ejecta and regolith is believed to originate from the Pythagoras crater (2.68 Ga) located to the north and >600 km away from CE-5 sampling site (Qian, Xiao, Wang, et al., 2021; Xie et al., 2020), and importantly, some Mg-suite rocks identified in the CE-5 samples are interpreted to represent materials ejected from Pythagoras (He et al., 2024). Consequently, it is possible that the zircon fragment investigated here was delivered to the CE-5 landing site as a part of ejecta from Pythagoras and was excavated and recycled to the CE-5 landing site via a younger impact in the Em4/P58 area (Qian, Xiao, Head, Wöhler, et al., 2021).

The highlands materials closest to the landing site (∼15 km away) are represented by kipukas interpreted to represent Iridum ejecta (Qian, Xiao, Head, Bogert, et al., 2021), which in turn probably recycles a significant proportion of material from Imbrium basin ejecta. Further afield (∼100 km away), Montes Jura is also interpreted as a mixture of Iridum and Imbrium ejecta (Qian, Xiao, Head, Bogert, et al., 2021; Qiao et al., 2014). Therefore, some of the Mg-suite rock fragments in the CE-5 soil can reflect a complex history of recycling of material ejected by multiple impacts but ultimately originating from the Imbrium basin, taking into account that many Apollo breccias are interpreted as Imbrium ejecta and contain similar rock fragments (Liu et al., 2012; Nemchin et al., 2008). A number of craters, such as Mairan (3.50 Ga), Harpalus (2.40 Ga), Sharp, Sharp B (1.15 Ga), and Aristarchus (0.16 Ga) (Xie et al., 2020), located at the northern to north-eastern to eastern fringes of Oceanus Procellarum (Figure 6), and even more distant Kepler (625–950 Ma) and Copernicus (796 Ma) (Qian, Xiao, Head, Bogert, et al., 2021), have been suggested to contribute ejecta to the regolith near CE-5 landing site (Fu et al., 2021; Hou et al., 2022; Qian, Xiao, Head, Bogert, et al., 2021) and therefore can be viewed as formed by impacts responsible for the final delivery of exotic materials including Mg-suite fragments. Some of these impacts, which are younger than the Imbrium impact (Nemchin et al., 2021; Snape et al., 2016), can recycle earlier ejecta mostly from the Imbrium basin, while others could potentially contain primary outcrops of Mg-suite rocks in their target and deliver them to the CE-5 landing site. These outcrops, for instance, some olivine-rich and Mg-spinel outcrops have been identified by remote sensing on both lunar nearside and farside (Dhingra et al., 2011; Isaacson et al., 2011; Klima et al., 2011, 2013; Moriarty et al., 2021; Pieters et al., 2011), including the northern and western edges of the Imbrium basin.

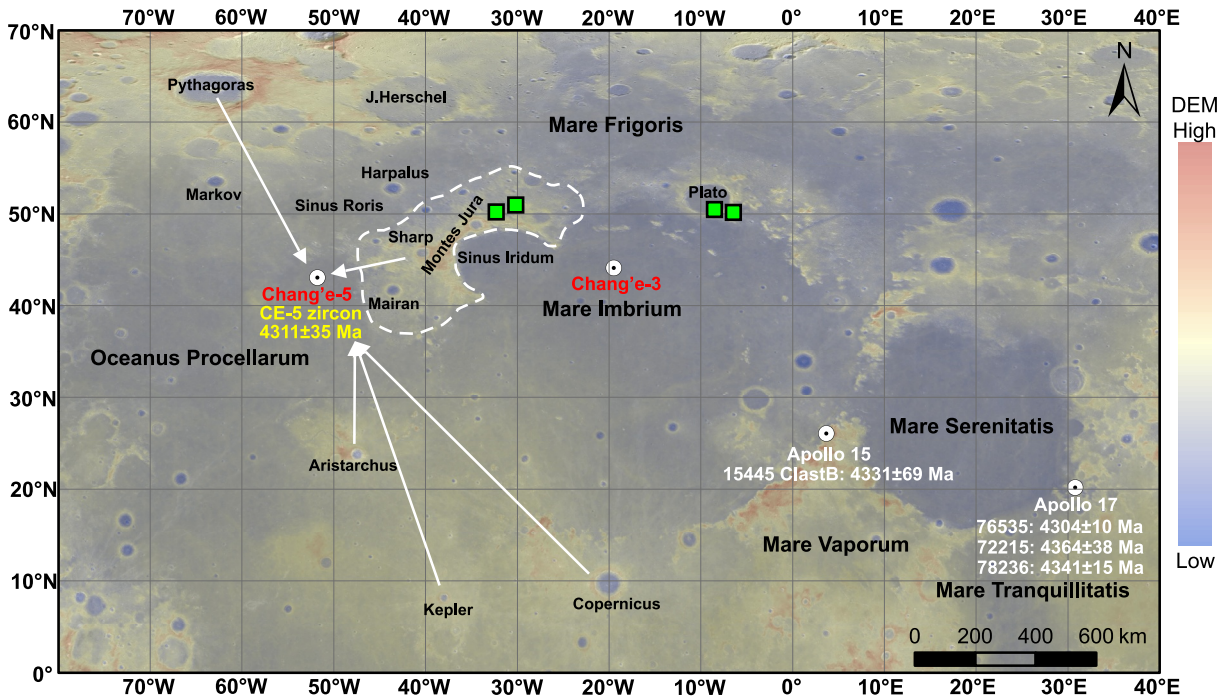

Figure 6. Possible regions of origin of investigated zircon illustrated using Chang'e-1 CCD map showing Chang'e-5 sampling site and adjacent areas. The digital elevation model (DEM) is presented using different colors, with red representing high and blue representing low. Some of the Apollo sampling sites and the ages of the Mg-suite rocks that occur at these sites are labeled on the map (Borg & Carlson, 2023). The green squares represent Mg-suite rocks identified by remote sensing observations in the northern part of Mare Imbrium (Klima et al., 2011). Solid white arrows mark the possible transportation direction of highlands materials. The white dashed line provides the boundaries of the highlands in the north-eastern part of Oceanus Procellarum. Chang'e-1 global images are from CNSA (2019a, 2019b).

4.3. Insights Into Early Lunar Magmatism

Important implication of discovering 4,311 ± 35 Ma zircon grain that can be linked to Mg-suite host in CE-5 soil, irrespective of whether it represents a multistage recycling through multiple impacts or direct delivery from the target containing these rocks, is that the original location of Mg-suite rocks is likely to be to the northwest or southwest of Imbrium basin, in contrast to Apollo samples that originate from south-eastern side of the basin distributed in the low and middle latitudes of the nearside (Barboni et al., 2024; Borg & Carlson, 2023; Borg et al., 2020). Consequently, the presence of Mg-suite fragments in CE-5 soil confirms remote sensing observations indicating wide distribution of these rocks through PKT (He et al., 2024). The zircon age obtained here also provides the first direct evidence that Mg-suite magmatism could have been a contemporaneous event occurring across a vast area on the near side of the Moon and perhaps even over the entire Moon. In addition, the zircon ages further corroborate the 4.3 Ga zircon age peak on the Moon (Barboni et al., 2024; Borg & Carlson, 2023; Borg et al., 2015). This coincidence of ages, as well as the overlap with the timing of the early lunar crust construction, may reflect extensive magmatism throughout the Moon during this period.

5. Conclusions

An ancient zircon grain was found in agglutinate in the CE-5 lunar regolith. SIMS U-Pb dating indicates an age of 4,311 ± 35 Ma for this zircon, distinguishing it from younger local basalts. The chemistry of this zircon indicates that its parent magma is likely to be anhydrous, Mg-rich, and low-viscosity. The REE concentrations observed in this zircon fall within the range of other lunar zircons, and the REE concentrations of parent melt calculated from the zircon's REE fall within the range of Mg- and Alkali-suite rocks. We infer that the host rock of this zircon is more likely to be Mg-suites, although we cannot rule out the possibility of Alkali-suites.

A more plausible explanation for the mechanism of zircon delivery to the CE-5 sampling site is that zircon was transported from the highlands near CE-5 landing site by an impact into one of these highlands' regions or a series of impacts starting with an initial impact into the highlands target. The likelihood of directly excavating ancient lunar crustal material underlying the Em4 basalt is low, given the thickness of the basaltic lava flows. Regardless

of the exact delivery mechanism, the discovery of 4.3 Ga lunar zircon at the CE-5 sampling site further corroborates the lunar 4.3 Ga magmatic event, suggesting that the formation of Mg-suite rocks may be contemporaneous and widespread on at least the nearside of the moon.

Data Availability Statement

All data used in this paper are available in Ding et al. (2025). Chang'e-1 global images are available in CNSA (2019a, 2019b).

Acknowledgments
We thank the CNSA for providing the lunar sample CE5C0600YJFM00501. We thank the Chang'e-1 payload team for mission operations and CNSA for providing the Chang'e-1 data that made this study possible. We are grateful to Juan Li (NJU) for SEM analysis and Kexin Xu (NJU) for EPMA analysis. We are grateful to Steven Simon, one anonymous reviewer and editor Jean-Pierre Williams for their constructive comments. This work was financially supported by the National Natural Science Foundation of China (Grants 42025202 and 42241121 X.-L. W.) and the State Key Laboratory of Critical Earth Material Cycling and Mineral Deposits, Nanjing University.

References

Barboni, M., Szymanowski, D., Schoene, B., Dauphas, N., Zhang, Z. J., Chen, X., & McKeegan, K. D. (2024). High-precision U-Pb zircon dating identifies a major magmatic event on the Moon at 4.338 Ga. *Science Advances*, *10*(30), eadn9871. https://doi.org/10.1126/sciadv.adn9871

Bellucci, J. J., Nemchin, A. A., Grange, M., Robinson, K. L., Collins, G., Whitehouse, M. J., et al. (2019). Terrestrial-like zircon in a clast from an Apollo 14 breccia. *Earth and Planetary Science Letters*, *510*, 173–185. https://doi.org/10.1016/j.epsl.2019.01.010

Black, L. P., Kamo, S. L., Allen, C. M., Davis, D. W., Aleinikoff, J. N., Valley, J. W., et al. (2004). Improved $^{206}Pb/^{238}U$ microprobe geochronology by the monitoring of a trace-element-related matrix effect; SHRIMP, ID–TIMS, ELA–ICP–MS and oxygen isotope documentation for a series of zircon standards. *Chemical Geology*, *205*(1), 115–140. https://doi.org/10.1016/j.chemgeo.2004.01.003

Borg, L. E., & Carlson, R. W. (2023). The evolving chronology of Moon formation. *Annual Review of Earth and Planetary Sciences*, *51*(1), 25–52. https://doi.org/10.1146/annurev-earth-031621-060538

Borg, L. E., Cassata, W. S., Wimpenny, J., Gaffney, A. M., & Shearer, C. K. (2020). The formation and evolution of the Moon's crust inferred from the Sm-Nd isotopic systematics of highlands rocks. *Geochimica et Cosmochimica Acta*, *290*, 312–332. https://doi.org/10.1016/j.gca.2020.09.013

Borg, L. E., Gaffney, A. M., & Shearer, C. K. (2015). A review of lunar chronology revealing a preponderance of 4.34–4.37 Ga ages. *Meteoritics & Planetary Sciences*, *50*(4), 715–732. https://doi.org/10.1111/maps.12373

Boschi, S., Wang, X.-L., Hui, H., Yin, Z., Guan, Y., Hu, H., et al. (2023). Compositional variability of 2.0-Ga lunar basalts at the Chang'e-5 landing site. *Journal of Geophysical Research: Planets*, *128*(5), e2022JE007627. https://doi.org/10.1029/2022JE007627

Carley, T. L., Bell, E. A., Miller, C. F., Claiborne, L. L., Hunt, A., Kirkpatrick, H. M., & Harrison, T. M. (2022). Zircon-modeled melts shed light on the formation of Earth's crust from the Hadean to the Archean. *Geology*, *50*(9), 1028–1032. https://doi.org/10.1130/G50017.1

Carlson, R. W., & Lugmair, G. W. (1981). Sm-Nd age of lherzolite 67667: Implications for the processes involved in lunar crustal formation. *Earth and Planetary Science Letters*, *56*, 1–8. https://doi.org/10.1016/0012-821X(81)90112-6

Che, X., Nemchin, A., Liu, D., Long, T., Wang, C., Norman, M. D., et al. (2021). Age and composition of young basalts on the Moon, measured from samples returned by Chang'e-5. *Science*, *374*(6569), 887–890. https://doi.org/10.1126/science.abl7957

CNSA. (2019a). Chang'E-1 global digital elevation model with 500m resolution dataset [Dataset]. *Ground Research and Application System of China's Lunar and Planetary Exploration Program*. https://doi.org/10.12350/CLPDS.GRAS.CE1.DEM-500m.vA

CNSA. (2019b). Chang'E-1 global digital orthophoto model with 120m resolution dataset [Dataset]. *Ground Research and Application System of China's Lunar and Planetary Exploration Program*. https://doi.org/10.12350/CLPDS.GRAS.CE1.DOM-120m.vA

Coble, M. A., Vazquez, J. A., Barth, A. P., Wooden, J., Burns, D., Kylander-Clark, A., et al. (2018). Trace element characterisation of MAD-559 zircon reference material for ion microprobe analysis. *Geostandards and Geoanalytical Research*, *42*(4), 481–497. https://doi.org/10.1111/ggr.12238

Crow, C. A., McKeegan, K. D., & Moser, D. E. (2017). Coordinated U–Pb geochronology, trace element, Ti-in-zircon thermometry and microstructural analysis of Apollo zircons. *Geochimica et Cosmochimica Acta*, *202*, 264–284. https://doi.org/10.1016/j.gca.2016.12.019

Dhingra, D., Pieters, C. M., Boardman, J. W., Head, J. W., Isaacson, P. J., & Taylor, L. A. (2011). Compositional diversity at Theophilus Crater: Understanding the geological context of Mg-spinel bearing central peaks. *Geophysical Research Letters*, *38*(11). https://doi.org/10.1029/2011GL047314

Dickinson, J. E., & Hess, P. C. (1982). Zircon saturation in lunar basalts and granites. *Earth and Planetary Science Letters*, *57*(2), 336–344. https://doi.org/10.1016/0012-821X(82)90154-6

Ding, C., Nemchin, A., Wang, X., Guan, Y., Tian, L., & Xie, W. (2025). Attachment data for "Evidence of 4.3 Ga Mg-suite magmatism in the western Procellarum KREEP Terrane provided by zircon from Chang'e-5 regolith" [Dataset]. *figshare*. https://doi.org/10.6084/m9.figshare.28189088.v1

Dymek, R. F., Albee, A. L., & Chodos, A. A. (1975). Comparative petrology of lunar cumulate rocks of possible primary origin: Dunite 72415, troctolite 76535, norite 78235, and anorthosite 62237. In *Paper Presented at the 6th Lunar and Planetary Science Conference, Houston, United States*.

Elardo, S. M., & Astudillo Manosalva, D. F. (2023). Complexity and ambiguity in the relationships between major lunar crustal lithologies and meteoritic clasts inferred from major and trace element modeling. *Geochimica et Cosmochimica Acta*, *354*, 13–26. https://doi.org/10.1016/j.gca.2023.05.020

Elardo, S. M., Draper, D. S., & Shearer, C. K. (2011). Lunar Magma Ocean crystallization revisited: Bulk composition, early cumulate mineralogy, and the source regions of the highlands Mg-suite. *Geochimica et Cosmochimica Acta*, *75*(11), 3024–3045. https://doi.org/10.1016/j.gca.2011.02.033

Elardo, S. M., Laneuville, M., McCubbin, F. M., & Shearer, C. K. (2020). Early crust building enhanced on the Moon's nearside by mantle melting-point depression. *Nature Geoscience*, *13*(5), 339–343. https://doi.org/10.1038/s41561-020-0559-4

Fu, X., Hou, X., Zhang, J., Li, B., Ling, Z., Jolliff, B. L., et al. (2021). Possible non-mare lithologies in the regolith at the Chang'E-5 landing site: Evidence from remote sensing data. *Journal of Geophysical Research: Planets*, *126*(5), e2020JE006797. https://doi.org/10.1029/2020JE006797

Grange, M. L., Nemchin, A. A., & Pidgeon, R. T. (2013). The effect of 1.9 and 1.4 Ga impact events on 4.3 Ga zircon and phosphate from an Apollo 15 melt breccia. *Journal of Geophysical Research: Planets*, *118*(10), 2180–2197. https://doi.org/10.1002/jgre.20167

Grange, M. L., Pidgeon, R. T., Nemchin, A. A., Timms, N. E., & Meyer, C. (2013). Interpreting U–Pb data from primary and secondary features in lunar zircon. *Geochimica et Cosmochimica Acta*, *101*, 112–132. https://doi.org/10.1016/j.gca.2012.10.013

Gross, J., Hilton, A., Prissel, T. C., Setera, J. B., Korotev, R. L., & Calzada-Diaz, A. (2020). Geochemistry and petrogenesis of northwest Africa 10401: A new type of the Mg-suite rocks. *Journal of Geophysical Research: Planets*, *125*(5), e2019JE006225. https://doi.org/10.1029/2019JE006225

Harrison, T. M., & Schmitt, A. K. (2007). High sensitivity mapping of Ti distributions in Hadean zircons. *Earth and Planetary Science Letters*, *261*(1), 9–19. https://doi.org/10.1016/j.epsl.2007.05.016

He, Q., Cao, Z., Qian, Y., Hui, H., Baziotis, I., Xiao, L., et al. (2024). Petrogenesis of magnesian troctolitic granulite clasts from Chang'e-5 drilling sample: Implications for the origin of ejecta material from lunar highlands. *Icarus*, *408*, 115853. https://doi.org/10.1016/j.icarus.2023.115853

Hess, P. C. (1994). Petrogenesis of lunar troctolites. *Journal of Geophysical Research*, *99*(E9), 19083–19093. https://doi.org/10.1029/94JE01868

Hinton, R. W., & Upton, B. G. J. (1991). The chemistry of zircon: Variations within and between large crystals from syenite and alkali basalt xenoliths. *Geochimica et Cosmochimica Acta*, *55*(11), 3287–3302. https://doi.org/10.1016/0016-7037(91)90489-R

Hoskin, P. W. O., & Schaltegger, U. (2003). The composition of zircon and igneous and metamorphic petrogenesis. *Reviews in Mineralogy and Geochemistry*, *53*(1), 27–62. https://doi.org/10.2113/0530027

Hou, X., Fu, X., Qiao, L., Li, B., Yin, C., Zhang, J., & Ling, Z. (2022). Absolute model ages of three craters in the vicinity of the Chang'E-5 landing site and their geologic implications. *Icarus*, *372*, 114730. https://doi.org/10.1016/j.icarus.2021.114730

Hu, Z., Li, X.-H., Luo, T., Zhang, W., Crowley, J., Li, Q., et al. (2021). Tanz zircon megacrysts: A new zircon reference material for the microbeam determination of U–Pb ages and Zr–O isotopes. *Journal of Analytical Atomic Spectrometry*, *36*(12), 2715–2734. https://doi.org/10.1039/D1JA00311A

Isaacson, P. J., Pieters, C. M., Besse, S., Clark, R. N., Head, J. W., Klima, R. L., et al. (2011). Remote compositional analysis of lunar olivine-rich lithologies with Moon Mineralogy Mapper (M3) spectra. *Journal of Geophysical Research*, *116*(E6), E00G11. https://doi.org/10.1029/2010JE003731

Jochum, K. P., Nohl, U., Herwig, K., Lammel, E., Stoll, B., & Hofmann, A. W. (2005). GeoReM: A new geochemical database for reference materials and isotopic standards. *Geostandards and Geoanalytical Research*, *29*(3), 333–338. https://doi.org/10.1111/j.1751-908X.2005.tb00904.x

Jolliff, B. L., Haskin, L. A., Colson, R. O., & Wadhwa, M. (1993). Partitioning in REE-saturating minerals: Theory, experiment, and modelling of whitlockite, apatite, and evolution of lunar residual magmas. *Geochimica et Cosmochimica Acta*, *57*(16), 4069–4094. https://doi.org/10.1016/0016-7037(93)90354-Y

Keller, C. B., Boehnke, P., & Schoene, B. (2017). Temporal variation in relative zircon abundance throughout Earth history. *Geochemical Perspectives Letters*, *3*, 179–189. https://doi.org/10.7185/geochemlet.1721

Klima, R. L., Cahill, J., Hagerty, J., & Lawrence, D. (2013). Remote detection of magmatic water in bullialdus crater on the Moon. *Nature Geoscience*, *6*(9), 737–741. https://doi.org/10.1038/ngeo1909

Klima, R. L., Pieters, C. M., Boardman, J. W., Green, R. O., Head, J. W., III., Isaacson, P. J., et al. (2011). New insights into lunar petrology: Distribution and composition of prominent low-Ca pyroxene exposures as observed by the Moon Mineralogy Mapper (M3). *Journal of Geophysical Research*, *116*(E6), E00G06. https://doi.org/10.1029/2010JE003719

Korotev, R. L., Jolliff, B. L., Zeigler, R. A., Seddio, S. M., & Haskin, L. A. (2011). Apollo 12 revisited. *Geochimica et Cosmochimica Acta*, *75*(6), 1540–1573. https://doi.org/10.1016/j.gca.2010.12.018

Li, C., Hu, H., Yang, M.-F., Pei, Z.-Y., Zhou, Q., Ren, X., et al. (2022). Characteristics of the lunar samples returned by the Chang'E-5 mission. *National Science Review*, *9*(2), nwab188. https://doi.org/10.1093/nsr/nwab188

Li, Q.-L., Zhou, Q., Liu, Y., Xiao, Z., Lin, Y., Li, J.-H., et al. (2021). Two-billion-year-old volcanism on the Moon from Chang'e-5 basalts. *Nature*, *600*(7887), 54–58. https://doi.org/10.1038/s41586-021-04100-2

Liu, D., Jolliff, B. L., Zeigler, R. A., Korotev, R. L., Wan, Y., Xie, H., et al. (2012). Comparative zircon U–Pb geochronology of impact melt breccias from Apollo 12 and lunar meteorite SaU 169, and implications for the age of the Imbrium impact. *Earth and Planetary Science Letters*, *319–320*, 277–286. https://doi.org/10.1016/j.epsl.2011.12.014

Longhi, J., & Boudreau, A. E. (1979). Complex igneous processes and the formation of the primitive lunar crustal rocks. In *Paper Presented at the 10th Lunar and Planetary Science Conference, Houston, United States*.

Mattinson, J. M., Graubard, C. M., Parkinson, D. L., & McClelland, W. C. (1996). U-Pb Reverse discordance in zircons: The Role of Fine-scale oscillatory zoning and Sub-Micron Transport of Pb. In A. Basu & S. Hart (Eds.), *Earth processes: Reading the isotopic code*, *Geophysical Monograph series* (Vol. 95, pp. 355–370). American Geophysical Union. https://doi.org/10.1029/GM095p0355

McDonough, W. F., & Sun, S.-S. (1995). The composition of the Earth. *Chemical Geology*, *120*(3–4), 223–253. https://doi.org/10.1016/0009-2541(94)00140-4

Meyer, C., Galindo, C., Jr., & Yang, V. (1991). Lunar zircon. In *Paper Presented at the 22nd Lunar and Planetary Science Conference, Houston, United States*.

Meyer, C., Williams, I. S., & Compston, W. (1996). Uranium-lead ages for lunar zircons: Evidence for a prolonged period of granophyre formation from 4.32 to 3.88 Ga. *Meteoritics & Planetary Sciences*, *31*(3), 370–387. https://doi.org/10.1111/j.1945-5100.1996.tb02075.x

Moriarty, D. P., Dygert, N., Valencia, S. N., Watkins, R. N., & Petro, N. E. (2021). The search for lunar mantle rocks exposed on the surface of the Moon. *Nature Communications*, *12*(1), 4659. https://doi.org/10.1038/s41467-021-24626-3

Nemchin, A. A., Grange, M. L., & Pidgeon, R. T. (2010). Distribution of rare earth elements in lunar zircon. *American Mineralogist*, *95*(2–3), 273–283. https://doi.org/10.2138/am.2010.3297

Nemchin, A. A., Long, T., Jolliff, B. L., Wan, Y., Snape, J. F., Zeigler, R., et al. (2021). Ages of lunar impact breccias: Limits for timing of the Imbrium impact. *Geochemistry*, *81*(1), 125683. https://doi.org/10.1016/j.chemer.2020.125683

Nemchin, A. A., Pidgeon, R. T., Whitehouse, M. J., Vaughan, J. P., & Meyer, C. (2008). SIMS U–Pb study of zircon from Apollo 14 and 17 breccias: Implications for the evolution of lunar KREEP. *Geochimica et Cosmochimica Acta*, *72*(2), 668–689. https://doi.org/10.1016/j.gca.2007.11.009

Nemchin, A. A., Timms, N., Pidgeon, R. T., Geisler, T., Reddy, S., & Meyer, C. (2009). Timing of crystallization of the lunar magma ocean constrained by the oldest zircon. *Nature Geoscience*, *2*(2), 133–136. https://doi.org/10.1038/ngeo417

Papike, J. J., Fowler, G. W., Shearer, C. K., & Layne, G. D. (1996). Ion microprobe investigation of plagioclase and orthopyroxene from lunar Mg-suite norites: Implications for calculating parental melt REE concentrations and for assessing postcrystallization REE redistribution. *Geochimica et Cosmochimica Acta*, *60*(20), 3967–3978. https://doi.org/10.1016/0016-7037(96)00212-8

Papike, J. J., Ryder, G., & Shearer, C. (1998). Lunar samples. In J. J. Papike (Ed.), *Planetary materials, reviews in mineralogy and geochemistry* (Vol. 36, pp. 5-001–5-234). The Mineralogical Society of America.

Papike, J. J., Simon, S. B., & Laul, J. C. (1982). The lunar regolith: Chemistry, mineralogy, and petrology. *Reviews of Geophysics*, *20*(4), 761–826. https://doi.org/10.1029/RG020i004p00761

Pidgeon, R. T., Nemchin, A. A., van Bronswijk, W., Geisler, T., Meyer, C., Compston, W., & Williams, I. S. (2007). Complex history of a zircon aggregate from lunar breccia 73235. *Geochimica et Cosmochimica Acta*, *71*(5), 1370–1381. https://doi.org/10.1016/j.gca.2006.11.021

Pieters, C. M., Besse, S., Boardman, J., Buratti, B., Cheek, L., Clark, R. N., et al. (2011). Mg-spinel lithology: A new rock type on the lunar farside. *Journal of Geophysical Research*, *116*(E6), E00G08. https://doi.org/10.1029/2010JE003727

Qian, Y., Xiao, L., Head, J. W., van der Bogert, C. H., Hiesinger, H., & Wilson, L. (2021). Young lunar mare basalts in the Chang'e-5 sample return region, northern Oceanus Procellarum. *Earth and Planetary Science Letters*, *555*, 116702. https://doi.org/10.1016/j.epsl.2020.116702

Qian, Y., Xiao, L., Head, J. W., Wöhler, C., Bugiolacchi, R., Wilhelm, T., et al. (2021). Copernican-aged (<200 Ma) impact ejecta at the Chang'e-5 landing site: Statistical evidence from crater morphology, morphometry, and degradation models. *Geophysical Research Letters*, *48*(20), e2021GL095341. https://doi.org/10.1029/2021GL095341

Qian, Y., Xiao, L., Wang, Q., Head, J. W., Yang, R., Kang, Y., et al. (2021). China's Chang'e-5 landing site: Geology, stratigraphy, and provenance of materials. *Earth and Planetary Science Letters*, *561*, 116855. https://doi.org/10.1016/j.epsl.2021.116855

Qiao, L., Xiao, L., Zhao, J., Huang, Q., & Haruyama, J. (2014). Geological features and evolution history of Sinus Iridum, the Moon. *Planetary and Space Science*, *101*, 37–52. https://doi.org/10.1016/j.pss.2014.06.007

Raedeke, L. D., & Mccallum, I. S. (1984). Investigations in the stillwater complex: Part II. Petrology and petrogenesis of the ultramafic series. *Journal of Petrology*, *25*(2), 395–420. https://doi.org/10.1093/petrology/25.2.395

Shearer, C. K., Elardo, S. M., Petro, N. E., Borg, L. E., & McCubbin, F. M. (2015). Origin of the lunar highlands Mg-Suite: An integrated petrology, geochemistry, chronology, and remote sensing perspective. *American Mineralogist*, *100*(1), 294–325. https://doi.org/10.2138/am-2015-4817

Shearer, C. K., & Papike, J. J. (2005). Early crustal building processes on the moon: Models for the petrogenesis of the magnesian suite. *Geochimica et Cosmochimica Acta*, *69*(13), 3445–3461. https://doi.org/10.1016/j.gca.2005.02.025

Shervais, J. W., & McGee, J. J. (1999). KREEP cumulates in the western lunar highlands; ion and electron microprobe study of alkali-suite anorthosites and norites from Apollo 12 and 14. *American Mineralogist*, *84*(5–6), 806–820. https://doi.org/10.2138/am-1999-5-616

Shih, C.-Y., Nyquist, L. E., Bogard, D. D., Wooden, J. L., Bansal, B. M., & Wiesmann, H. (1985). Chronology and petrogenesis of a 1.8 G lunar granitic clast:14321,1062. *Geochimica et Cosmochimica Acta*, *49*(2), 411–426. https://doi.org/10.1016/0016-7037(85)90033-X

Simon, S. B., Papike, J. J., Gosselin, D. C., & Laul, J. C. (1985). Petrology and chemistry of Apollo 12 regolith breccias. *Journal of Geophysical Research*, *90*(S01), 75–86. https://doi.org/10.1029/JB090iS01p00075

Simon, S. B., Papike, J. J., Laul, J. C., Hughes, S. S., & Schmitt, R. A. (1988). Apollo 16 regolith breccias and soils: Recorders of exotic component addition to the Descartes region of the moon. *Earth and Planetary Science Letters*, *89*(2), 147–162. https://doi.org/10.1016/0012-821X(88)90167-7

Simon, S. B., Papike, J. J., Shearer, C. K., & Laul, J. C. (1983). Petrology of the Apollo 11 highland component. *Journal of Geophysical Research*, *88*(S01), B103–B138. https://doi.org/10.1029/JB088iS01p0B103

Snape, J. F., Nemchin, A. A., Grange, M. L., Bellucci, J. J., Thiessen, F., & Whitehouse, M. J. (2016). Phosphate ages in Apollo 14 breccias: Resolving multiple impact events with high precision U–Pb SIMS analyses. *Geochimica et Cosmochimica Acta*, *174*, 13–29. https://doi.org/10.1016/j.gca.2015.11.005

Snyder, G. A., Taylor, L. A., & Halliday, A. N. (1995). Chronology and petrogenesis of the lunar highlands alkali suite: Cumulates from KREEP basalt crystallization. *Geochimica et Cosmochimica Acta*, *59*(6), 1185–1203. https://doi.org/10.1016/0016-7037(95)00034-W

Stacey, J. S., & Kramers, J. D. (1975). Approximation of terrestrial lead isotope evolution by a two-stage model. *Earth and Planetary Science Letters*, *26*(2), 207–221. https://doi.org/10.1016/0012-821X(75)90088-6

Taylor, S. R., Norman, M. D., & Esat, T. M. (1993). The Mg-suite and the highland crust: An unsolved enigma. In *Paper Presented at the 24th Lunar and Planetary Science Conference, Houston, United States*.

Thiessen, F., Nemchin, A. A., Snape, J. F., & Whitehouse, M. J. (2019). U-Pb SIMS ages of Apollo 14 zircon: Identifying distinct magmatic episodes. *Meteoritics & Planetary Sciences*, *54*(8), 1720–1736. https://doi.org/10.1111/maps.13310

Tian, H.-C., Wang, H., Chen, Y., Yang, W., Zhou, Q., Zhang, C., et al. (2021). Non-KREEP origin for Chang'e-5 basalts in the Procellarum KREEP Terrane. *Nature*, *600*(7887), 59–63. https://doi.org/10.1038/s41586-021-04119-5

Tian, H.-C., Yang, W., Zhang, D., Zhang, H., Jia, L., Wu, S., et al. (2023). Petrogenesis of Chang'E-5 mare basalts: Clues from the trace elements in plagioclase. *American Mineralogist*, *108*(9), 1669–1677. https://doi.org/10.2138/am-2022-8570

Trail, D., Barboni, M., & McKeegan, K. D. (2020). Evidence for diverse lunar melt compositions and mixing of the pre-3.9 Ga crust from zircon chemistry. *Geochimica et Cosmochimica Acta*, *284*, 173–195. https://doi.org/10.1016/j.gca.2020.06.018

Vanderliek, D. M., Becker, H., & Rocholl, A. (2021). Impact-related crystallization and modification of small zircons in Apollo 15 and 16 impactites at 4.2 Ga. *Earth and Planetary Science Letters*, *576*, 117216. https://doi.org/10.1016/j.epsl.2021.117216

Warren, P. H., & Wasson, J. T. (1978). Compositional-petrographic investigation of pristine nonmare rocks. In *Paper Presented at the 9th Lunar and Planetary Science Conference, Houston, United States*.

Watson, E. B., & Harrison, T. M. (2005). Zircon thermometer reveals minimum melting Conditions on earliest Earth. *Science*, *308*(5723), 841–844. https://doi.org/10.1126/science.1110873

Wiedenbeck, M., Allé, P., Corfu, F., Griffin, W. L., Meier, M., Oberli, F., et al. (1995). Three natural zircon standards for U-Th-Pb, Lu-Hf, trace element and REE analyses. *Geostandards Newsletter*, *19*(1), 1–23. https://doi.org/10.1111/j.1751-908X.1995.tb00147.x

Xie, M., Xiao, Z., Zhang, X., & Xu, A. (2020). The provenance of regolith at the Chang'e-5 candidate landing region. *Journal of Geophysical Research: Planets*, *125*(5), e2019JE006112. https://doi.org/10.1029/2019JE006112

Zeng, X., Joy, K. H., Li, S., Lin, Y., Wang, N., Li, X., et al. (2020). Oldest immiscible silica-rich melt on the Moon recorded in a ~4.38 Ga zircon. *Geophysical Research Letters*, *47*(4), e2019GL085997. https://doi.org/10.1029/2019GL085997

Zeng, X., Li, X., & Liu, J. (2023). Exotic clasts in Chang'e-5 regolith indicative of unexplored terrane on the Moon. *Nature Astronomy*, *7*(2), 152–159. https://doi.org/10.1038/s41550-022-01840-7

Zhang, A.-C., Hsu, W.-B., Li, X.-H., Ming, H.-L., Li, Q.-L., Liu, Y., & Tang, G.-Q. (2011). Impact melting of lunar meteorite Dhofar 458: Evidence from polycrystalline texture and decomposition of zircon. *Meteoritics & Planetary Sciences*, *46*(1), 103–115. https://doi.org/10.1111/j.1945-5100.2010.01144.x

Zhang, A.-C., Taylor, L. A., Wang, R.-C., Li, Q.-L., Li, X.-H., Patchen, A. D., & Liu, Y. (2012). Thermal history of Apollo 12 granite and KREEP-rich rock: Clues from Pb/Pb ages of zircon in lunar breccia 12013. *Geochimica et Cosmochimica Acta*, *95*, 1–14. https://doi.org/10.1016/j.gca.2012.07.023

Zhang, B., Lin, Y., Moser, D. E., Hao, J., Liu, Y., Zhang, J., et al. (2021). Radiogenic Pb mobilization induced by shock metamorphism of zircons in the Apollo 72255 Civet Cat norite clast. *Geochimica et Cosmochimica Acta*, *302*, 175–192. https://doi.org/10.1016/j.gca.2021.03.012

Zhang, B., Lin, Y., Moser, D. E., Warren, P. H., Hao, J., Barker, I. R., et al. (2021). Timing of lunar Mg-suite magmatism constrained by SIMS U-Pb dating of Apollo norite 78238. *Earth and Planetary Science Letters*, *569*, 117046. https://doi.org/10.1016/j.epsl.2021.117046

Zhou, Q., Liu, Y., Yang, S., Li, Q.-L., Chen, Y., Zhang, G., et al. (2023). The youngest lunar zircon reveals an extremely fractionated nature of Chang'e-5 basalt. *Geochimica et Cosmochimica Acta*, *358*, 126–133. https://doi.org/10.1016/j.gca.2023.08.017

Zong, K., Wang, Z., Li, J., He, Q., Li, Y., Becker, H., et al. (2022). Bulk compositions of the Chang'E-5 lunar soil: Insights into chemical homogeneity, exotic addition, and origin of landing site basalts. *Geochimica et Cosmochimica Acta*, *335*, 284–296. https://doi.org/10.1016/j.gca.2022.06.037